



HAL
open science

Characterization of the heme oxygenase protein family in *Arabidopsis thaliana* reveals a diversity of functions

Bjoern Gisk, Yukiko Yasui, Takayuki Kohchi, Nicole Frankenberg-Dinkel

► To cite this version:

Bjoern Gisk, Yukiko Yasui, Takayuki Kohchi, Nicole Frankenberg-Dinkel. Characterization of the heme oxygenase protein family in *Arabidopsis thaliana* reveals a diversity of functions. *Biochemical Journal*, 2009, 425 (2), pp.425-434. 10.1042/BJ20090775 . hal-00479198

HAL Id: hal-00479198

<https://hal.science/hal-00479198>

Submitted on 30 Apr 2010

HAL is a multi-disciplinary open access archive for the deposit and dissemination of scientific research documents, whether they are published or not. The documents may come from teaching and research institutions in France or abroad, or from public or private research centers.

L'archive ouverte pluridisciplinaire **HAL**, est destinée au dépôt et à la diffusion de documents scientifiques de niveau recherche, publiés ou non, émanant des établissements d'enseignement et de recherche français ou étrangers, des laboratoires publics ou privés.

Characterization of the heme oxygenase protein family in *Arabidopsis thaliana* reveals a diversity of functions

Bjoern Gisk¹, Yukiko Yasui², Takayuki Kohchi² and Nicole Frankenberg-Dinkel^{1*}

¹Physiology of Microorganisms, Ruhr-University Bochum, Universitaetsstr. 150, 44780 Bochum, Germany

²Graduate School of Biostudies, Kyoto University, Kyoto 606-8502, Japan

Running title: *Arabidopsis* heme oxygenases

Key words: heme oxygenase, HO2, biliverdin, protoporphyrin IX, *Arabidopsis thaliana*

Abbreviations used: BV, biliverdin; DCIP, dichloroindophenol; DCMU, dichlorophenyldimethylurea ; Fd, ferredoxin; GFP, green fluorescent protein; HO, heme oxygenase; PΦB, phytychromobilin; proto IX, protoporphyrin IX

***Corresponding author**

Nicole Frankenberg-Dinkel
Physiology of Microorganisms
Ruhr-University Bochum
Universitaetsstr. 150
44780 Bochum
Germany
Phone: +49 234 3223101
Fax: +49 234 3214620
Email: nicole.frankenberg@rub.de

SYNOPSIS

Heme oxygenases (HOs) catalyze the oxidative cleavage of heme to biliverdin, iron and carbon monoxide. In plants, the product of the reaction is biliverdin IX α , the precursor of the phytochrome chromophore and is thus essential for proper photomorphogenesis. *Arabidopsis thaliana* contains one major biochemically characterized HO (HY1) and three additional putative HOs (HO2, HO3 and HO4). All four proteins are encoded in the nucleus but contain chloroplast translocation sequences at their N-termini. The transit peptides of all four proteins are sufficient for chloroplast translocalisation as shown by GFP reporter gene fusions. Overall, all four proteins can be divided into two subfamilies: HO1 and HO2. Here we show that all members of the HO1 subfamily (HY1, HO3, and HO4) are active monomeric HOs and convert heme to biliverdin IX α using spinach ferredoxin as an electron donor. Addition of a second electron donor like ascorbate led to ten time faster heme conversion. Furthermore, heme turnover is also promoted by light when spinach thylakoids are present. All HO1 family members displayed similar kinetic parameters indicating a possible involvement in phytochrome chromophore biosynthesis by all of them. HO2 did not yield sufficient amounts of soluble protein and therefore required the construction of a synthetic gene adapted to the codon usage of *E. coli*. HO2 is unable to bind or degrade heme and therefore it is not a heme oxygenase. However, HO2 shows strong binding of protoporphyrin IX, a precursor of both, heme and chlorophyll biosynthesis. A possible function of HO2 in the regulation of tetrapyrrole metabolism is discussed.

INTRODUCTION

Light is one of the most essential factors for plant growth and development. In order to sense light a variety of photoreceptors, spanning nearly the entire visible and UV region of the spectrum have evolved. Sensing of red/ far-red light is mediated via phytochromes which are able to photoisomerize between two stable conformations, the red-light absorbing Pr-form and the far-red-light absorbing Pfr-form. This photoconversion between the two spectrally distinct forms is mediated by a covalently bound open-chain tetrapyrrole (bilin), which is phytychromobilin (PΦB) in plants. In *Arabidopsis thaliana* the phytochrome superfamily consists of five members (PHYA-E) which have different functions in growth and development [1].

While the biosynthesis of the apo-phytochrome occurs in the cytosol, the biosynthesis of PΦB takes place in the chloroplast [1]. An early precursor of PΦB is protoporphyrin IX (proto IX) which is located at the branch point of heme- and chlorophyll biosynthesis [2]. At this point Mg^{2+} is inserted by magnesium chelatase to ultimately yield chlorophyll, whereas ferrochelatase inserts Fe^{2+} to generate heme which is the direct precursor of all bilins. Cleavage of heme by heme oxygenase (HO; E.C. 1.14.99.3) subsequently yields the first open-chain product biliverdin (BV) IX α . Heme degradation requires three molecules of molecular oxygen and seven electrons and results in formation of BV IX α , carbon monoxide, and Fe^{2+} via the intermediates α -meso-hydroxyheme, α -verdoheme, and the iron(III)-BV IX α complex (Figure 1) [3]. BV IX α is subsequently reduced by PΦB synthase (HY2), a member of the ferredoxin-dependent bilin reductases, to yield 3Z-PΦB [4, 5]. Next, PΦB is transported out of the plastid and assembles with the apo-phytochrome in an autocatalytic reaction to form functional holo-phytochrome. 3Z-PΦB is most likely isomerized to the 3E-isomer prior to the assembly with apo-phytochrome in the cytosol. Whether the 3Z- or the 3E-isomer (or both) is transported out of the chloroplast is currently unknown. While there is a single gene encoding PΦB synthase in *A. thaliana* [4], four putative HO genes have been identified [6].

The four HOs of *A. thaliana* cluster into two subfamilies: the HO1 subfamily and the HO2 subfamily. While HY1 (HO1), HO3, and HO4 belong to the HO1 subfamily solely HO2 is a member of the HO2 subfamily. Both HO subfamilies are also present in other plant species like soybean, tomato, sorghum, rice and pine [6, 7]. The main difference between these two subfamilies is an inserted spacer sequence in the HO2 subfamily of ~ 34-55 amino acid residues which is rich in glutamate, aspartate and glycine residues. Furthermore, all members of the HO2 family lack the conserved histidine residue in the active site that is involved in heme-iron coordination in the HO1 family [6]. However, phenotypic analysis of the *ho2-1* mutant in *Arabidopsis* suggested that HO2 also contributes to proper photomorphogenesis [6]. Some of the observed phenotypes resemble that of the *hy1-100* mutant but to a lesser extent. Phenotypes observed include hypocotyl elongation under red and far-red light, smaller rosette leaves and chlorosis. Moreover, a slower degradation rate after red light irradiation of PHYA was observed indicating a mixed (apo- and holo-) PHYA pool in the *ho2-1* mutant [6]. Therefore, loss of HO2 might limit the availability of PΦB.

All four *A. thaliana* HO genes are transcribed but with different expression levels. While *HY1* shows the highest expression level followed by *HO2*, the expression of *HO3* and *HO4* is extremely low but detectable [8, 9]. In addition, gene expression profiling revealed that *HO2* expression is slightly induced by light at the onset of greening, whereas *HY1*, *HO3* and *HO4* are constitutively expressed [9]. While the main function of plant HOs seems to be the biosynthesis of the phytochrome chromophore, mammalian HOs are involved in oxidative stress response, iron utilization and show potent anti-inflammatory effects [10-12]. Here, three isoforms exist, HO-1, HO-2 and HO-3. HO-3 is an isoform with low catalytic activity and

unknown physiological function [13]. HO-2 on the other hand is constitutively expressed and thought to be mostly involved in signaling pathways. HO-1 expression is induced by oxidative stress as the HO reaction product BV or the subsequent reduction product bilirubin has antioxidant function [14]. Recent reports on a HO from soybean also suggest a function in oxidative stress response in plants [15, 16]. However, mammalian and plant HOs seem to differ in the use of the required reductant. Mammalian HOs were shown to use NADPH-cytochrome P450 reductase (NADPH-cytochrome *c* reductase) [17-19] as the preferred reductant whereas plant, cyanobacterial and bacterial HOs seem to prefer ferredoxin (Fd) [20-23]. In addition, plant HOs appear to require a second reductant such as ascorbate for full activity [21].

The most common open-chain product of the HO reaction is BV IX α resulting from the oxidative cleavage of heme at the α -meso carbon bridge. Yet, several recent reports prove the existence of HOs with alternative cleavage sites resulting in the three other BV isomers IX β , γ and δ [24, 25]. The regiospecificity of these HOs cannot be predicted from primary amino acid sequence or crystal structures but rather seems to be due to a different orientation of the heme substrate in the active site pocket as shown for the β - and δ -specific HO (PigA) from *Pseudomonas aeruginosa* [26, 27].

Until now, HY1 is the only biochemically characterized HO from *A. thaliana* [21]. The functionality of HO3 and HO4 was only indirectly proven by co-expression of the HOs with the apo-phytochrome from *Deinococcus radiodurans* (DrBphP) which resulted in the binding of the HO reaction product BV to the phytochrome [8]. Whether HO2 is a true HO has not been biochemically addressed at all due to low expression rates and solubility issues. However, the phenotype at least points towards a function within tetrapyrrole metabolism. Here we present biochemical data giving new insights into the function of all four *A. thaliana* HOs. For the first time we were able to obtain sufficient amounts of recombinant HO2 by using a codon optimized synthetic gene. Interestingly, HO2 is not able to bind or convert heme and is therefore not a heme oxygenase. However, strong binding of proto IX points towards a role of HO2 in tetrapyrrole metabolism.

EXPERIMENTAL

Chemicals

All chemicals were purchased from Sigma (Munich, Germany) and were ACS grade or better. HPLC-grade acetone and 80% formic acid were purchased from Mallinckrodt Baker (Griesheim, Germany).

Subcellular localization experiments with green fluorescent protein fusions

The coding regions for the putative transit peptide for HY1 (HO1), HO2, HO3, and HO4 were amplified from *Arabidopsis* (Columbia) cDNA with the HY1 primers (5'-CGGGATCCCACCATGGCGTATTTAGCTCCGA-3', 5'-CCGCTCGAGGCAGTAGTAGCCGCAACCA-3'), the HO2 primers (5'-CGGGATCCCACCATGGCTTCTCTTCTCAGGC-3', 5'-CCGCTCGAGTGTGAGGCCTTTTGTGTGA-3'), the HO3 primers (5'-CGGGATCCCACCATGGCTACAACAAGACTTAAC-3', 5'-CCGCTCGAGATAGCCGCCGAGTCACC-3'), and the HO4 primers (5'-CGGGATCCCACCATGGCTACATCAAGACTTAATGC-3', 5'-CCGCTCGAGGCCACAACATTCACCACCA-3'), respectively. The amplified DNA fragments were digested with *Bam*HI and *Xho*I and then cloned into the corresponding sites of pENTRTM1A (Invitrogen) to have the entry clones. The entry clone for intact green fluorescent protein (GFP) was prepared by self-ligation of pENTRTM1A digested with *Xmn*I-

EcoRV. After verification of the orientation and the nucleotide sequences, a recombination reaction was performed between the entry clones and the destination vector pGWB5 [28] using LR Clonase (Invitrogen) to generate an in-frame fusion with the GFP gene under the CaMV35S promoter. The plasmid pGWB42-MIRO1TM for the mitochondrial marker YFP-MIRO1 [29] was obtained from Dr. Yamaoka (University of Tokyo). The transient assays of fluorescent protein expression in *Nicotiana benthamiana* were performed according to [30] by using *Agrobacterium tumefaciens* C58C1 pGV2260. After 36 hr co-cultivation in the dark, the signals for GFP and chloroplast autofluorescence were examined under a confocal microscope (FluoView 1000, Olympus).

Construction of HO2 expression vector

A synthetic gene encoding the mature (without the predicted transit peptide sequence) HO2 was adapted to the codon bias of *Escherichia coli* genes to provide a successful expression. The synthetic gene *HO2_{syn}* of 738 bp was assembled from synthetic oligonucleotides (GENEART GmbH, Regensburg, Germany) with addition of a 5' *Bam*HI and a 3' *Xho*I restriction site, respectively. After cleavage with the respective enzymes the artificial gene was cloned into pGEX-6P-1 to generate pGEX-mHO2. The synthetic DNA sequence has been deposited in Genbank under the accession number FJ854354.

Expression and purification of recombinant HOs

HY1 was produced and purified using the plasmid pGEX-mHY1 as described before [31] with minor modifications. The purified HY1 was dialyzed against 100 mM potassium phosphate buffer pH 7.2. The same protocol was used for the expression and purification of mHO2_{syn} except that this GST-fusion has a recognition sequence for PreScission Protease instead of Thrombin.

The pET24a-mHO3 and pET24a-mHO4 plasmids for recombinant C-terminal hexahistidine-tagged mature (without the predicted transit peptide) HO3 and HO4 production were kindly provided by Dr. R. D. Vierstra (University of Wisconsin, Madison, USA). An overview of the employed constructs is given in Figure 3A.

For production of recombinant HO3 and HO4, 2 liters of LB media containing 50 mg/ml kanamycin were inoculated 1:100 from an overnight culture of *E. coli* BL21 (DE3) carrying the respective plasmid constructs and grown at 37 °C to OD_{578nm} ~0.6-0.8. After a temperature shift to 17 °C, protein production was induced by the addition of 125 µM isopropyl-β-D-thiogalactopyranoside, and cells were cultured for additional 15 h at 180 rpm. Afterwards cells were harvested by centrifugation and stored at -20 °C. Cell lysis and disruption was the same as described before [31]. The supernatant was loaded on a Talon[®] cobalt affinity chromatography column. Washing and elution steps were done according to instructions supplied by the manufacturer (Clontech-Takara Bio Europe, Saint-Germain-en-Laye, France). Proteins were eluted with a buffer containing 75 mM imidazole. The protein solutions were pooled and dialyzed against reaction buffer (100 mM potassium phosphate, pH 7.2).

Analysis of the quaternary structure using gel permeation chromatography

The oligomerization state of the four enzymes was investigated using analytical gel permeation chromatography. A Superdex[™] 75 HR10/30 column (GE Healthcare, Munich, Germany) equilibrated with 100 mM potassium phosphate, pH 7.2, at a flow rate of 0.5 ml/min, was employed. Protein was monitored at 280 nm using the UV-900 detector of an AEKTA-explorer system (GE Healthcare). Standard proteins with known molecular weight were used to generate a calibration curve (apoferritin 443.000; β-amylase 200.000; alcohol dehydrogenase 150.000; albumin 66.000; carboanhydrase 29.000 und cytochrome c 12.400) from which the quaternary structure was calculated.

Reconstitution and titration of heme oxygenases with heme

15 mg of crystalline hemin was dissolved in 5 mL dimethylsulfoxid (DMSO) to generate a 4.6 mM hemin solution. Hemin was added to the purified HOs to give a final 2:1 heme:protein ratio. The sample was subsequently applied to a hydroxylapatite column (1.0 x 2.0 cm) which was equilibrated with 10 mM potassium phosphate buffer (pH 7.2). The column was then washed with the same buffer until no more free heme could be detected spectrophotometrically, and the protein eluted with 100 mM potassium phosphate buffer (pH 7.2). The fractions containing detectable heme-HO complex ($OD_{280nm} + OD_{405nm}$) were pooled and concentrated using a VIVASPIN[®] (Vivascience, Goettingen, Germany) concentrator at 40,000×g. The concentration of recombinantly produced HOs was determined using the molar extinction coefficient (ϵ_{280nm}) calculated from the deduced amino acid composition [32].

Titration of HOs with heme was monitored by absorption spectroscopy. Aliquots of heme (0.58-10.0 μ M) were added to the cuvette containing 5 μ M HO at 25 °C. Spectra were recorded 5 min after heme addition. The same heme concentrations were added to a sample cuvette containing only buffer. The K_D value was obtained from the difference spectra of free heme and protein bound heme at 405 nm.

Determination of the extinction coefficient for the heme-HO complexes

The millimolar extinction coefficient at 405 nm for the heme-HO complex was determined using the pyridine hemochrome method [33]. The isolated heme-HO complex (10 μ M) was converted to a pyridine-hemochrome in a 500 μ l sample volume by addition of 62.5 μ l pyridine and 62.5 μ l of 0.5 M NaOH solution. The spectrum of the oxidized pyridine hemochrome was recorded. After addition of an excess of dithionite the spectrum of the reduced ferrous pyridine hemochrome was recorded. The difference spectrum of the reduced and oxidized form was calculated at 557 nm. The concentration of heme was determined from the extinction coefficient using an $\epsilon_{405nm} = 34.530 \text{ mM}^{-1} \text{ cm}^{-1}$.

Heme oxygenase assay

Heme oxygenase activity was measured in 500 μ l final volume containing 10 μ M HO, 10 μ M heme, 0.15 mg/ml bovine serum albumin, 4.6 μ M Fd (spinach), 0.025 unit/ml spinach Fd-NADP⁺ oxidoreductase and 10 μ M catalase from *Aspergillus niger* in 100 mM potassium phosphate buffer (pH 7.2).

The reaction was started by addition of an NADPH-regenerating system containing 6.5 mM glucose 6-phosphate, 0.82 mM NADP⁺, and 1.1 unit/ml glucose-6-phosphate dehydrogenase. Spectral changes between 300 and 900 nm were monitored for 30 min at 25 °C using an Agilent Technologies 8453 UV-visible Spectroscopy system. Sodium ascorbate and/ or desferrioxamine were added to a final concentration of 5 mM unless otherwise noted. The rate of BV IX α formation at 25°C was calculated using the absorbance change at 670 nm. The concentration of BV IX α was estimated using an extinction coefficient at 670 nm of 6.25 $\text{mM}^{-1} \text{ cm}^{-1}$ in 100 mM potassium phosphate buffer (pH 7.2) determined from published values of other solvents [34]. K_m values were calculated for the HOs using Eadie Hofstee and Lineweaver Burk plots. Therefore, the standard assay with 10 μ M HO and varied heme concentrations between 1 μ M and 100 μ M were used. Temperature dependence of the HO reaction was measured between 10 °C and 45 °C. The activation energy (E_A) was calculated based on an Arrhenius plot. The pH dependence of the reaction was monitored between pH 5.0 and 9.0 in 100 mM potassium phosphate buffer. For all assays the standard conditions as described above were used.

Isolation of thylakoid membrane and heme oxygenase assay

Fresh spinach leaves (25 g) were added to 35 ml digestion buffer (0.4 M sucrose, 20 mM KCl, 0.5 mM KH_2PO_4 , 50 mM Tris, pH 7.6) and homogenized for 5 min. The homogenized leaves were then filtered through a fleece cloth and the filtrate centrifuged for 5 min at 40,000×g. The pellet was resuspended in 10 ml digestion buffer. After a second centrifugation step at 40,000 ×g for 5 min the pellet was resuspended in 5 ml buffer (0.66 M sucrose, 40 mM KCl, 3 mM KH_2PO_4 , 4 mM MgCl_2 , 100 mM HEPES, pH 8.0) and 5 ml H_2O . The chlorophyll content of these crude membranes was calculated as described before [35]. For the HO assay 10 μM HO-heme complex was incubated with 0.15 mg/ml bovine serum albumin, 4.6 μM Fd (spinach), 5 mM sodium ascorbate, 5 mM tiron, and isolated thylakoid membranes (10 μg of chlorophyll) in 100 mM potassium phosphate buffer (pH 7.2) either in the dark or for 100 s in the dark followed by irradiation for 200 s with 460 W m^{-2} of actinic white light. Absorbance was measured at 680 nm and HO activity was calculated by the rate of absorbance change at this wavelength. The reaction was inhibited with 50 μM dichlorophenyl dimethylurea (DCMU) or 50 μM DCMU and 200 μM reduced dichloroindophenol (DCIP). DCIP was reduced using 0.1 mM HCl and 5 mM ascorbate prior to use.

HPLC analysis of heme oxygenase reaction products

HOs assay mixtures were acidified with tenfold 0.1% trifluoroacetic acid (TFA) and loaded onto a Waters (Milford, MA, USA) C18- Sep-Pak Light cartridge preconditioned as follows: 3 ml acetonitrile to wet the Sep-Pak, 3 ml MilliQ water, 3 ml 0.1% TFA, 3 ml 10% methanol in 0.1% TFA, 3 ml acetonitrile, 3 ml MilliQ water, 3 ml 10% methanol in TFA. After the sample was loaded onto the Sep-Pak, it was washed with 6 ml 0.1% TFA, and 6 ml 20% methanol / 80 % TFA (0.1%). The tetrapyrroles were then eluted from the Sep-Pak using 1 ml of 100% acetonitrile. The eluate was dried using a Speed-Vac lyophilizer, and dried samples were analyzed by HPLC. Samples were first dissolved in 10 μl DMSO and then diluted in 150 μl of the HPLC mobile phase. Following brief centrifugation and filtration through a 0.45 μm polytetrafluoroethylene syringe filter, tetrapyrroles were analyzed with reversed phase chromatography using an Agilent Technologies 1100 liquid chromatograph. The HPLC column used for all analyses was a 4.6 x 250 mm Phenomenex Ultracarb 5 μm OD20 analytical column with a 4.6 x 30 mm guard column of the same material. The mobile phase consisted of acetone:20 mM formic acid (50:50 by volume), and the flow rate was 0.6 ml/min. Eluates were monitored at 650 nm and 380 nm using an Agilent Technologies 1100 series diode array detector. As needed, complete spectra were obtained for the peaks desired. Peak areas were quantified using Agilent Technologies Chemstation software.

RESULTS

HO2, HO3 and HO4 are localized to the plastid

The HY1 protein contained a functional transit peptide for plastid localization and is processed to the mature plastid heme oxygenase [21, 31]. The amino termini of HO2, HO3 and HO4 deduced from cDNA sequences also showed features of a transit peptide by the ChloroP program [36]; <http://www.cbs.dtu.dk/services/ChloroP/>). The conservation of primary sequences in this region is much lower than in the heme oxygenase region, indicating that the stretches in the amino termini are transit peptides. To show the function of the putative transit peptides experimentally, we fused the potential transit peptide regions of all four *Arabidopsis* HO genes to a gene encoding green fluorescent protein (GFP) from jellyfish under the control of the cauliflower mosaic virus 35S promoter. The constructs were

introduced to *Nicotiana benthamiana* by Agroinfection [30]. The GFP fluorescence in oval structures was observed in the samples in which HY1 (HO1), HO2, HO3 and HO4 constructs were introduced (Figure 2 a, d, g and j). These signals matched the chloroplast autofluorescence (chlorophyll channel; Figure 2 b, e, h, and k; merge in Figure 2 c, f, i, l), demonstrating that the fusion protein is efficiently targeted to chloroplasts. A control construct without the putative transit peptide showed GFP fluorescence throughout the cytoplasm (Figure 2 m) that is clearly different from the red autofluorescence from chlorophyll in chloroplasts (Figure 2 n and o). The findings of functional transit peptides in the deduced HY1, HO2, HO3 and HO4 sequences imply that the proteins encoded by *HY1*, *HO2*, *HO3* and *HO4* are present as the processed mature protein in the plastid compartment. As heme is also present in mitochondria, mitochondrial localization was observed by the mitochondrial marker MIRO1 [29]. The yellow fluorescent protein (YFP) signals for MIRO1 are different from those of HY1 to HO4 (Figure 2 p). There is no indication for a mitochondrial localization of HO1 to HO4 in this analysis.

Expression and purification of recombinant heme oxygenases

The *A. thaliana* HO genes *HY1*, *HO2*, *HO3*, and *HO4* were expressed without their predicted chloroplast transit peptides either using a *tac* promoter-driven N-terminal GST fusion expression system (*HY1*, *HO2*) [21] or the pET vector system (*HO3*, *HO4*) using a T7-promoter and a His-tag fusion (Figure 3A) [8]. After induction with isopropyl- β -D-thiogalactopyranoside and expression over night at 17 °C the *Escherichia coli* BL21 (DE3) cells had a brownish color (except cells expressing HO2; data not shown). This is in contrast to the expression of bacterial or mammalian HOs in *E. coli* which most often show a green color, because of BV accumulation in the cells [23, 37-39]. Therefore, the lack of green color implies that the plant HOs might not be fully active in *E. coli*.

HY1 was expressed and purified as described before and yielded a major band migrating at ~ 27 kDa on SDS-PAGE [21]. Recombinant HO3 and HO4 contained a C-terminal hexahistidine-tag and were purified by cobalt affinity chromatography. This purification strategy led to over 90% purity (Figure 3B). The final yield of recombinant HY1, HO3, and HO4 from 1L bacterial culture was ~ 60 mg each. The proteins were stored on ice and stayed fully active for up to 4 days in 100 mM potassium phosphate buffer (pH 7.2). Unfortunately, the expression and purification of recombinant HO2 yielded only low amounts of soluble protein (Figure 3B, lane 2). Therefore, a synthetic gene (without the transit peptide coding region) adapted to the codon usage of *E. coli* K12 was generated and cloned into pGEX-6-P1. The yield from this synthetic construct was significantly higher than using the native gene (Figure 3B, lane 5) and resulted in ~ 24 mg recombinant HO2 from 1L bacterial culture. Since the recombinant protein migrated slightly slower than predicted in SDS-PAGE, the integrity of the recombinant protein was verified by tryptic digest followed by MALDI-TOF/TOF analysis (data not shown).

Arabidopsis heme oxygenases are monomeric enzymes

While the majority of HOs are monomeric enzymes, others like HO-2 from *Synechocystis* sp. PCC 6803 or HO-2 from human were shown to be dimeric [40-42]. To probe the oligomerisation state of *A. thaliana* HOs, gel permeation chromatography on a SuperdexTM 75 HR10/30 column was performed.

All four HO proteins eluted at ~ 11.5 ml as a major symmetric peak. However, while HY1 and HO3 showed no aggregation after purification, HO4 also displayed a minor peak at ~ 8.5 ml which was shown to be aggregated protein by SDS-PAGE (data not shown). HO2 on the other hand displayed two minor peaks at ~15 ml and 18 ml which are most likely degradation

products. Under our experimental conditions and in comparison to the elution profile of standard proteins all four investigated recombinant HOs are monomeric.

HO2 from Arabidopsis does not bind and convert heme

A. thaliana possesses four annotated HOs with only *hyl* and *ho2* mutants showing strong defects in photomorphogenesis, raising the question whether the HOs differ with regard to enzyme activity. Thus, in a first attempted we analyzed the heme binding properties of the four HOs.

The formation of the heme-HO complex was determined by absorption spectroscopy. Interestingly, only the three HOs belonging to the HO1 subfamily displayed a strong Soret band at 405 nm indicating enzyme bound heme (Figure 4A, C, D). This Soret band is identical to that reported for HOs from other sources [21, 43-45]. Incubation of HO2 with heme did not result in a significant absorbance change or in the formation of a distinct Soret band (Figure 4B). Even after extended incubation time, no heme binding was observed. The addition of reductant (Fd) also had no influence on the heme binding behavior (data not shown). As HO2 is not able to bind heme, no heme binding constant (K_D) and no activity could be determined. For the heme-binding HOs from the HO1 subfamily the K_D -values were calculated from titration data determined by difference absorption spectroscopy (data not shown). All three HO1 subfamily members have K_D -values in the micromolar range. While HY1 displayed the highest affinity with approximately 1.6 μM (in agreement with [21]), HO3 and HO4 had slightly weaker affinities with 2.3 μM and 2.8 μM , respectively (Table 1). All three HOs appeared to be saturated at a ratio of 1:1 heme to protein.

Extinction coefficients of the recombinant HOs were determined using the method of Berry and Trumpower [33]. For HY1 a value of 203 $\text{mM}^{-1} \text{cm}^{-1}$ was determined, for HO3 271 $\text{mM}^{-1} \text{cm}^{-1}$ and of HO4 175 $\text{mM}^{-1} \text{cm}^{-1}$, respectively (Table 1).

HO2 binds the heme precursor protoporphyrin IX with high affinity

Since no heme binding of HO2 was observed we tested whether it will bind the structurally related heme precursor protoporphyrin IX (proto IX). Interestingly, not only HO2 but all HOs were able to bind proto IX (Figure 5A). But in contrast to the HOs of the HO1 subfamily, HO2 forms a stable complex with proto IX even during gel permeation chromatography (Figure 5B). Addition of reductant had no influence on the spectroscopic characteristics of the protoIX-HO2 complex.

Only HO1 subfamily HOs are true heme oxygenases

For enzymatic turnover heme was added to HY1, HO3, and HO4 at a 2:1 ratio and free heme was removed by hydroxyl apatite column chromatography. Addition of reduced spinach Fd to the heme-HO complexes resulted in the immediate formation of the ferrous dioxyheme complex [heme(Fe^{2+})- O_2], which was accompanied by shift in the Soret band from 405 nm to 410 nm and by the appearance of β -/ α -bands at 540 nm and 579 nm, respectively (Figure 4A). Within 30 min the ferrous dioxyheme complex was fully degraded to ferric-BV (Figure 4A), the latter being poorly detectable spectroscopically. Therefore, all subsequent assays for HO3 and HO4 contained the iron chelator desferrioxamine and a broad peak between 650 nm and 670 nm was observed indicating the formation of free BV (Figure 4C, D). Please note that under these conditions β -/ α -bands are not observed. Release of CO from the HOs was assayed by the addition of myoglobin to the HO assay which gave a characteristic CO-bound myoglobin spectrum [37] (data not shown).

Since HOs are regiospecific enzymes the reaction products can be one of the four possible BV isomers. It has been shown previously that the IX α isomer is the product of the HY1 reaction which is subsequently converted to the phytochrome chromophore 3Z-P Φ B by P Φ B synthase [4, 5, 21]. However, HOs with other regiospecificities are known from bacteria and insects

[24, 25]. Thus, the reaction products of the three *Arabidopsis* HOs were analyzed by HPLC. Like HY1, *Arabidopsis* HO3 and HO4 produce the BV IX α isomer with a retention time of about 20 min (Figure 6).

Kinetic parameters of the HO1 subfamily are comparable

The pH optimum for the HO activities was pH 7.0 for HO3 and pH 7.25 for HY1 and HO4 (Figure 7A). All three proteins are more active in the basic pH region than at acid pH values (Figure 7A). The pH optimum of HY1 is identical to the one previously determined [21]. The reaction rate of enzyme activity is increasing between 10 °C and 45 °C (Figure 7B). An Arrhenius plot was used to calculate the individual activation energies (E_A) for each reaction. While the E_A for the HY1 reaction is known to be 35.60 J mol⁻¹ [21], an activation energy of 14.78 J mol⁻¹ and 10.76 J mol⁻¹ was calculated for HO3 and HO4, respectively.

Kinetic parameter for purified HO3 and HO4 were estimated from Eadie Hofstee plots without ascorbate to slow the reaction (see below) (data not shown). K_M values of 2.7 μ M (HO3) and 5.7 μ M (HO4) were determined and are comparable to those of other HOs [46]. For HY1, a K_M value of 1.3 μ M was published earlier [21].

Heme turnover is significantly increased by addition of a second reductant

A second reductant is known to increase enzyme activity of cyanobacterial and algal HOs as well as HY1 [21, 22, 47]. We therefore tested the effect of ascorbate on HO3 and HO4 turnover. For both enzymes, turnover of heme is ten-fold faster than without ascorbate (shown for HO3 in Figure 8). Under fast assay conditions with ascorbate the ferrous dioxyheme complex is not visible (Figure 8).

Ferredoxin is most likely the in vivo electron donor for the HO1 subfamily

For HY1 it was demonstrated that the primary electron donor *in vivo* is Fd [21]. Since all *A. thaliana* HOs possess a transit peptide sequence and were shown to be localized to the chloroplast (see Figure 2), Fd receiving electrons from photosystem I (PSI) is likely the natural electron donor for all of them. Addition of isolated thylakoid membranes to the HO assay significantly increased heme cleavage to BV after illumination (Figure 9A). In the presence of the electron transport inhibitor dichlorophenylmethylurea (DCMU) the BV formation decreases to a relative activity of about 20 % (Figure 9B). In this scenario cyclic electron flow does not result in net reduced Fd and subsequently heme turnover. Addition of reduced 2,6-dichlorophenolindophenol (DCIP) an artificial electron donor to the DCMU blocked assay resulted in an increased BV formation as reduced DCIP is able to reduce PSI.

DISCUSSION

Although the HO1 and HO2 subfamilies in *Arabidopsis* have been identified a couple of years ago direct evidence for the functionality of the individual members was lacking [6, 8, 31, 48]. Here we provide the first biochemical data for all four *Arabidopsis* annotated HOs using recombinant enzymes. While HY1 appears to be the key HO responsible for phytochrome chromophore biosynthesis, HO3 and HO4 are also classical α -hydroxylating HOs. Analysis of major biochemical parameters established that their activity does not significantly differ from that of HY1.

The mechanism of heme cleavage is conserved between HOs of the HO1 subfamily from *A. thaliana*, mammals and bacteria. Heme degradation results in production of BV IX α , CO and iron. Interestingly, higher plant HOs form a strong ferric-BV complex and an iron chelator (e.g. desferrioxamine) is essential to release BV *in vitro* (Figure 4C, D). This phenomenon has

also been observed earlier for HY1 from *Arabidopsis* [21] and HO from *Cyandium caladanium* [49]. As ~90 % of cellular iron is located in the chloroplast [50] it seems likely that the ferric-BV complex is not released spontaneously by HOs. One might hypothesize that only the interaction between HO and PΦB synthase (HY2) releases BV which is in turn converted by HY2 to PΦB.

Our experiments using isolated thylakoid membranes strongly support the role of Fd as the electron donor *in vivo* [21]. The genome of *A. thaliana* possesses a total of four Fd genes coding for three different types of [2Fe-2S] Fd: *AtFd1*, *AtFd2*, *AtFd3*, *AtFd4* [51]. These Fds can be divided into classic leaf type Fds (*AtFd1* and *AtFd2*), a root type Fd (*AtFd3*) and a high redox potential Fd (*AtFd4*). All Fds contain chloroplast transit peptides and are transported to the plastid. As predicted *Arabidopsis* HOs were shown to also localize to the chloroplast. Most likely one of the leaf type Fds is the natural redox partner for the HOs in photosynthetic cells [51]. However, in non-photosynthetic cells one of the other Fd is likely the natural electron donor. In this case, the Fd is reduced by NADPH generated by the oxidative pentose phosphate pathway.

The sole localization of all HOs to the plastid however raises the question how heme turnover outside the chloroplast is achieved. As mitochondria contain a large number of hemoproteins one would also postulate the presence of an active HO there. Although our experimental data did not show mitochondrial localization in *Nicotiana benthamiana*, we cannot exclude mitochondrial localization in *Arabidopsis*. In this regard, dual targeting of plant proteins to both the chloroplast and the mitochondria has been described [52]. Furthermore, another enzyme of the tetrapyrrole pathway, protoporphyrinogen oxidase of spinach, was shown to be localized to both compartments due to the use of two in-frame initiation codons [53].

A general phenomenon of higher plant HOs is that addition of ascorbate as a second reductant significantly influences heme turnover. Endogenous varying ascorbate levels might be a tool for modulating HO activity *in planta*. In this regard, it has been reported that the chloroplastidic ascorbate concentration can vary from 15-46 mM depending on light intensity with high light leading to increased ascorbate levels [54]. Therefore, HO activity is indirectly regulated by light through the levels of ascorbate ensuring sufficient phytochrome chromophore biosynthesis during the day. Furthermore, our biochemical data suggest a pH optimum for HO activities which are conform with the pH value of the stroma at night (pH 7.2) [55]. During the day the pH of the chloroplast increases to pH 8.0 which should decrease the activity of all three HOs. In contrast, HO enzyme activity increases with rising temperature. So the antagonistic dependency of HO activity on pH and temperature could be an additional tool to fine-tune HO activity.

Although it has been proposed earlier that HY1 is unable to use NADPH-cytochrome P450 reductase as a reductant, slow turnover of heme to the oxycomplex by HY1, HO3 and HO4 could be detected. Only further addition of ascorbate led to a complete turnover (data not shown). Therefore, it is rather unlikely that NADPH-cytochrome P450 reductase is a natural electron donor *in planta*.

Considering the weak mutant phenotype of *ho3* and *ho4* it appears that the enzymes do not have a large impact on phytochrome chromophore biosynthesis due to their low expression rates [8]. However, biochemical data suggest that they could completely substitute for HY1. Nevertheless, there is still the possibility that they might also function in oxidative stress response since the product of the reaction BV has reasonable antioxidant properties as shown for soybean nodules [15, 16]. Yet, there is currently no evidence that any of the HO genes in *A. thaliana* is inducible by oxidative- and/ or salt stress.

The most interesting result of this study however is the production and purification of soluble HO2 from a synthetic gene. This enabled us for the first time to address the question whether HO2 is indeed a HO. Our results clearly demonstrate that HO2 is unable to bind and degrade heme and raises the question of the function of this protein. Phenotypic analysis of the *ho2-1*

mutant plants suggested that HO2 also contributes to proper photomorphogenesis. This however does not necessarily demand a function in heme turnover. HO2 could have a different function in tetrapyrrole metabolism. One indication that HO2 is not a true HO is the absence of the conserved histidine residue in the active site that is usually involved in heme-iron coordination. This residue is replaced by an arginine in HO2. However, the sequence similarity (~38 %) suggests the same overall fold of all HOs including HO2 (except the inserted spacer sequence). It therefore was conceivable for us to test whether HO2 might bind heme precursors like proto IX. Interestingly, HO2 is able to bind proto IX with high affinity (stable complex during gel permeation chromatography, see Figure 5B). Although the three other *A. thaliana* HOs displayed the same binding behavior, proto IX in these enzymes can easily be replaced by heme indicating a high affinity to the natural substrate heme (data not shown). If the proto IX binding to HO2 is of any biological significance remains to be determined but we speculate that HO2 could either have a function as a proto IX storage protein to regulate tetrapyrrole flux through the pathway or that it might function as a carrier protein towards magnesium- and/ or ferrochelatase. In the future it will be necessary to analyze tetrapyrrole concentration in the chloroplasts in more detail to understand the role of the HOs from the HO1 and HO2 subfamily of *Arabidopsis*. Also the latter hypothesis should be addressed by protein-protein interaction studies which are currently under investigation. However, for the first time we could show that all three heme oxygenases of the HO1 subfamily are active HOs *in vitro* with nearly identical biochemical parameters and they are able to convert heme to BV IX_a. The member of the HO2 subfamily (HO2) is at this state of knowledge no true HO but might be involved in the regulation of the two tetrapyrrole biosynthetic pathways.

THIS IS NOT THE VERSION OF RECORD - see doi:10.1042/BJ20090775

Accepted Manuscript

Acknowledgements

We thank Drs. Yuuki Sakai and Takashi Araki for their support on the confocal microscope experiments, and Dr. Shohei Yamaoka for the MIRO1 plasmid and Dr. Richard D. Vierstra for the *HO2*, *HO3* and *HO4* expression clones. Thanks are also due to Dr. Lars I. Leichert for help with the MALDI-TOF/TOF analysis and Dr. Jessica Wiethaus and Andrea Busch for critical reading of the manuscript.

Funding

This work was supported by Teilprojekt C8 of the Sonderforschungsbereich 480 from the Deutsche Forschungsgemeinschaft to NFD and by the Grant-in-Aid for Scientific Research from the Japan Society for Promotion of Science to TK (21027021).

REFERENCES

- 1 Tu, S.-L. and Lagarias, J. C. (2005) The phytochromes. In *Handbook of Photosensory Receptors* (Briggs, W. and Spudich, J., eds.). pp. 121-149, Wiley-VCH, Weinheim
- 2 Frankenberg, N. and Lagarias, J. C. (2003) Biosynthesis and biological functions of bilins. In *The Porphyrin Handbook* (Kadish, K. M., Smith, K. M. and Guillard, R., eds.), Elsevier Science (USA)
- 3 Ortiz de Montellano, P. R. (2000) The mechanism of heme oxygenase. *Curr. Opin. Chem. Biol.* **4**, 221-227
- 4 Kohchi, T., Mukougawa, K., Frankenberg, N., Masuda, M., Yokota, A. and Lagarias, J. C. (2001) The Arabidopsis HY2 gene encodes phytochromobilin synthase, a ferredoxin-dependent biliverdin reductase. *Plant Cell.* **13**, 425-436
- 5 Frankenberg, N., Mukougawa, K., Kohchi, T. and Lagarias, J. C. (2001) Functional genomic analysis of the HY2 family of ferredoxin-dependent bilin reductases from oxygenic photosynthetic organisms. *Plant Cell.* **13**, 965-978
- 6 Davis, S. J., Bhoo, S. H., Durski, A. M., Walker, J. M. and Vierstra, R. D. (2001) The heme-oxygenase family required for phytochrome chromophore biosynthesis is necessary for proper photomorphogenesis in higher plants. *Plant Physiol.* **126**, 656-669
- 7 Terry, M. J., Linley, P. J. and Kohchi, T. (2002) Making light of it: the role of plant haem oxygenases in phytochrome chromophore synthesis. *Biochem Soc Trans.* **30**, 604-609
- 8 Emborg, T. J., Walker, J. M., Noh, B. and Vierstra, R. D. (2006) Multiple heme oxygenase family members contribute to the biosynthesis of the phytochrome chromophore in Arabidopsis. *Plant Physiol.* **140**, 856-868
- 9 Matsumoto, F., Obayashi, T., Sasaki-Sekimoto, Y., Ohta, H., Takamiya, K.-i. and Masuda, T. (2004) Gene Expression Profiling of the Tetrapyrrole Metabolic Pathway in Arabidopsis with a Mini-Array System. *Plant Physiol.* **135**, 2379-2391
- 10 Poss, K. D. and Tonegawa, S. (1997a) Heme oxygenase 1 is required for mammalian iron reutilization. *Proc. Natl. Acad. Sci. USA.* **94**, 10919-10924
- 11 Poss, K. D. and Tonegawa, S. (1997b) Reduced stress defense in heme oxygenase 1-deficient cells. *Proc. Natl. Acad. Sci. USA.* **94**, 10925-10930
- 12 Otterbein, L. E., Bach, F. H., Alam, J., Soares, M., Tao Lu, H., Wysk, M., Davis, R. J., Flavell, R. A. and Choi, A. M. (2000) Carbon monoxide has anti-inflammatory effects involving the mitogen-activated protein kinase pathway. *Nat Med.* **6**, 422-428
- 13 McCoubrey, W. K., Jr., Huang, T. J. and Maines, M. D. (1997) Isolation and characterization of a cDNA from the rat brain that encodes hemoprotein heme oxygenase-3. *Eur J Biochem.* **247**, 725-732
- 14 Maines, M. D., Trakshel, G. M. and Kutty, R. K. (1986) Characterization of two constitutive forms of rat liver microsomal heme oxygenase. Only one molecular species of the enzyme is inducible. *J Biol Chem.* **261**, 411-419
- 15 Balestrasse, K. B., Noriega, G. O., Batlle, A. and Tomaro, M. a. L. (2005) Involvement of heme oxygenase as antioxidant defense in soybean nodules. *Free Radical Research.* **39**, 145 - 151
- 16 Noriega, G. O., Balestrasse, K. B., Batlle, A. and Tomaro, M. L. (2004) Heme oxygenase exerts a protective role against oxidative stress in soybean leaves. *Biochem Biophys Res Commun.* **323**, 1003-1008
- 17 Tenhunen, R., Marver, H. S. and Schmid, R. (1969) Microsomal heme oxygenase. Characterization of the enzyme. *J Biol Chem.* **244**, 6388-6394
- 18 Yoshinaga, T., Sassa, S. and Kappas, A. (1982) The oxidative degradation of heme c by the microsomal heme oxygenase system. *J Biol Chem.* **257**, 7803-7807

- 19 Yoshinaga, T., Sassa, S. and Kappas, A. (1982) The occurrence of molecular interactions among NADPH-cytochrome c reductase, heme oxygenase, and biliverdin reductase in heme degradation. *J Biol Chem.* **257**, 7786-7793
- 20 Schacter, B. A., Nelson, E. B., Marver, H. S. and Masters, B. S. (1972) Immunochemical evidence for an association of heme oxygenase with the microsomal electron transport system. *J Biol Chem.* **247**, 3601-3607
- 21 Muramoto, T., Tsurui, N., Terry, M. J., Yokota, A. and Kohchi, T. (2002) Expression and biochemical properties of a ferredoxin-dependent heme oxygenase required for phytochrome chromophore synthesis. *Plant Physiol.* **130**, 1958-1966
- 22 Cornejo, J., Willows, R. D. and Beale, S. I. (1998) Phytobilin biosynthesis: cloning and expression of a gene encoding soluble ferredoxin-dependent heme oxygenase from *Synechocystis* sp. PCC 6803. *Plant J.* **15**, 99-107
- 23 Wegele, R., Tasler, R., Zeng, Y., Rivera, M. and Frankenberg-Dinkel, N. (2004) The heme oxygenase(s)-phytochrome system of *Pseudomonas aeruginosa*. *J Biol Chem.* **279**, 45791-45802
- 24 Paiva-Silva, G. O., Cruz-Oliveira, C., Nakayasu, E. S., Maya-Monteiro, C. M., Dunkov, B. C., Masuda, H., Almeida, I. C. and Oliveira, P. L. (2006) A heme-degradation pathway in a blood-sucking insect. *Proc Natl Acad Sci U S A.* **103**, 8030-8035
- 25 Ratliff, M., Zhu, W., Deshmukh, R., Wilks, A. and Stojiljkovic, I. (2001) Homologues of Neisserial Heme Oxygenase in Gram-Negative Bacteria: Degradation of Heme by the Product of the pigA Gene of *Pseudomonas aeruginosa*. *J. Bacteriol.* **183**, 6394-6403
- 26 Caignan, G. A., Deshmukh, R., Wilks, A., Zeng, Y., Huang, H. W., Moenne-Loccoz, P., Bunce, R. A., Eastman, M. A. and Rivera, M. (2002) Oxidation of heme to beta- and delta-biliverdin by *Pseudomonas aeruginosa* heme oxygenase as a consequence of an unusual seating of the heme. *J Am Chem Soc.* **124**, 14879-14892
- 27 Friedman, J., Lad, L., Li, H., Wilks, A. and Poulos, T. L. (2004) Structural basis for novel delta-regioselective heme oxygenation in the opportunistic pathogen *Pseudomonas aeruginosa*. *Biochemistry.* **43**, 5239-5245
- 28 Nakagawa, T., Kurose, T., Hino, T., Tanaka, K., Kawamukai, M., Niwa, Y., Toyooka, K., Matsuoka, K., Jinbo, T. and Kimura, T. (2007) Development of series of gateway binary vectors, pGWBs, for realizing efficient construction of fusion genes for plant transformation. *J Biosci Bioeng.* **104**, 34-41
- 29 Yamaoka, S. and Leaver, C. J. (2008) EMB2473/MIRO1, an Arabidopsis Miro GTPase, is required for embryogenesis and influences mitochondrial morphology in pollen. *Plant Cell.* **20**, 589-601
- 30 Voinnet, O., Rivas, S., Mestre, P. and Baulcombe, D. (2003) An enhanced transient expression system in plants based on suppression of gene silencing by the p19 protein of tomato bushy stunt virus. *Plant J.* **33**, 949-956
- 31 Muramoto, T., Kohchi, T., Yokota, A., Hwang, I. and Goodman, H. M. (1999) The Arabidopsis photomorphogenic mutant *hyl* is deficient in phytochrome chromophore biosynthesis as a result of a mutation in a plastid heme oxygenase. *Plant Cell.* **11**, 335-347.
- 32 Gill, S. C. and von Hippel, P. H. (1989) Calculation of protein extinction coefficients from amino acid sequence data. *Anal. Biochem.* **182**, 319-326
- 33 Berry, E. A. and Trumpower, B. L. (1987) Simultaneous determination of hemes a, b, and c from pyridine hemochrome spectra. *Anal. Biochem.* **161**, 1-15
- 34 Brindle, N. J., North, A. C. and Brown, S. B. (1986) Theoretical prediction and experimental measurement of the bile-pigment isomer pattern obtained from degradation of catalase haem. *Biochem. J.* **236**, 303-306
- 35 Arnon, D. I. and Whatley, F. R. (1949) Is chloride a coenzyme of photosynthesis? *Science.* **110**, 554-556

- 36 Emanuelsson, O., Nielsen, H. and von Heijne, G. (1999) ChloroP, a neural network-based method for predicting chloroplast transit peptides and their cleavage sites. *Protein Sci.* **8**, 978-984
- 37 Wilks, A. and Schmitt, M. P. (1998) Expression and characterization of a heme oxygenase (Hmu O) from *Corynebacterium diphtheriae*. Iron acquisition requires oxidative cleavage of the heme macrocycle. *J Biol Chem.* **273**, 837-841
- 38 Suzuki, T., Sato, M., Ishikawa, K. and Yoshida, T. (1992) Nucleotide sequence of cDNA for porcine heme oxygenase and its expression in *Escherichia coli*. *Biochem Int.* **28**, 887-893
- 39 Wilks, A. and Ortiz de Montellano, P. R. (1993) Rat liver heme oxygenase. High level expression of a truncated soluble form and nature of the meso-hydroxylating species. *J Biol Chem.* **268**, 22357-22362
- 40 Sato, H., Sugishima, M., Sakamoto, H., Higashimoto, Y., Shimokawa, C., Fukuyama, K., Palmer, G. and Noguchi, M. (2009) Crystal structure of rat haem oxygenase-1 in complex with ferrous verdohaem: presence of a hydrogen-bond network on the distal side. *Biochem. J.* **419**, 339-345
- 41 Bianchetti, C. M., Yi, L., Ragsdale, S. W. and Phillips, G. N., Jr. (2007) Comparison of apo- and heme-bound crystal structures of a truncated human heme oxygenase-2. *J Biol Chem.* **282**, 37624-37631
- 42 Sugishima, M., Hagiwara, Y., Zhang, X., Yoshida, T., Migita, C. T. and Fukuyama, K. (2005) Crystal structure of dimeric heme oxygenase-2 from *Synechocystis* sp. PCC 6803 in complex with heme. *Biochemistry.* **44**, 4257-4266
- 43 Gohya, T., Zhang, X., Yoshida, T. and Migita, C. T. (2006) Spectroscopic characterization of a higher plant heme oxygenase isoform-1 from *Glycine max* (soybean)--coordination structure of the heme complex and catabolism of heme. *FEBS J.* **273**, 5384-5399
- 44 Frankenberg-Dinkel, N. (2004) Bacterial heme oxygenases. *Antioxid Redox Signal.* **6**, 825-834
- 45 Wilks, A. (2002) Heme Oxygenase: Evolution, Structure and Mechanism. *Antiox. Redox Signal.* **4**, 603-614
- 46 Wilks, A., Black, S. M., Miller, W. L. and Ortiz de Montellano, P. R. (1995) Expression and characterization of truncated human heme oxygenase (hHO-1) and a fusion protein of hHO-1 with human cytochrome P450 reductase. *Biochemistry.* **34**, 4421-4427
- 47 Rhie, G. and Beale, S. I. (1992) Biosynthesis of phycobilins. Ferredoxin-supported NADPH-independent heme oxygenase and phycobilin-forming activities from *Cyanidium caldarium*. *J Biol Chem.* **267**, 16088-16093
- 48 Davis, S. J., Kurepa, J. and Vierstra, R. (1999) The *Arabidopsis thaliana* *HY1* locus, required for phytochrome-chromophore biosynthesis, encodes a protein related to heme oxygenases. *Proc. Natl. Acad. Sci. USA.* **96**, 6541-6546
- 49 Rhie, G. and Beale, S. I. (1995) Phycobilin biosynthesis: reductant requirements and product identification for heme oxygenase from *Cyanidium caldarium*. *Arch. Biochem. Biophys.* **320**, 182-194
- 50 Terry, N. and Abadia, J. (1986) Function of iron in chloroplasts. *Journal of Plant Nutrition.* **9**, 609 - 646
- 51 Hanke, G. T., Kimata-Arigo, Y., Taniguchi, I. and Hase, T. (2004) A post genomic characterization of *Arabidopsis* ferredoxins. *Plant Physiol.* **134**, 255-264
- 52 Peeters, N. and Small, I. (2001) Dual targeting to mitochondria and chloroplasts. *Biochimica et Biophysica Acta (BBA) - Molecular Cell Research.* **1541**, 54-63
- 53 Watanabe, N., Che, F. S., Iwano, M., Takayama, S., Yoshida, S. and Isogai, A. (2001) Dual targeting of spinach protoporphyrinogen oxidase II to mitochondria and chloroplasts by alternative use of two in-frame initiation codons. *J Biol Chem.* **276**, 20474-20481

- 54 Rautenkranz, A., Li, L., Machler, F., Martinoia, E. and Oertli, J. J. (1994) Transport of Ascorbic and Dehydroascorbic Acids across Protoplast and Vacuole Membranes Isolated from Barley (*Hordeum vulgare* L. cv Gerbel) Leaves. *Plant Physiol.* **106**, 187-193
- 55 Enser, U. and Heber, U. (1980) Metabolic regulation by pH gradients. Inhibition of photosynthesis by indirect proton transfer across the chloroplast envelope. *Biochim. Biophys. Acta.* **592**, 577-591

Accepted Manuscript

THIS IS NOT THE VERSION OF RECORD - see doi:10.1042/BJ20090775

FIGURE LEGENDS

Figure 1. Heme degradation as catalyzed by heme oxygenase (HO). Most HOs cleave heme at the α -meso carbon position yielding biliverdin IX α . This reaction requires seven electrons and three molecules molecular oxygen. Carbon monoxide and iron are released.

Figure 2. Subcellular localization of HY1, HO2, HO3 and HO4 by transient expression of the fused fluorescent proteins.

Microscopic images of GFP (a, d, g, j, m), YFP (p), chloroplast autofluorescence (b, e, h, k, n, q) and merge (c, f, i, l, o, r) from mesophyll cells of *Nicotiana benthamiana* infected with *Agrobacteria* harboring the GFP constructs. All images were taken at the same magnification. GFP fused to HY1 transit peptide (a, b, c), HO2 transit peptide (d, e, f), HO3 transit peptide (g, h, i), HO4 transit peptide (j, k, l). Images by intact GFP constructs (m, n, o) and by YFP fused to the transmembrane stretch of MIRO1 for mitochondria localization (p, q, r) are also shown. Bar: 20 μ m. All images were taken with a sensitive black-and-white camera and subsequently colored using the imaging software. YFP fluorescence was colored green for a better quality merge figure.

Figure 3. Purification of recombinant proteins. A. Scheme of the employed recombinant proteins. GST, glutathione-S-transferase; m, mature protein (lacking the predicted transit peptide sequence); numbers depict the amino acid residues in the full-length protein; syn, synthetic gene product, His₆, hexa-histidine tag. **B. Coomassie-stained SDS-PAGE of recombinant purified HOs.** Lane M: Molecular mass markers; lane 1: Purified HY1; lane 2: Purified HO2 (native gene); lane 3: Purified HO3; lane 4: Purified HO4; lane 5: Purified HO2 (synthetic gene adapted to *E.coli* codon usage) after cleavage with PreScission protease[®] and 2nd chromatography column. HY1 and HO2 were purified by GST-affinity chromatography followed by protease digestion and 2nd chromatography, HO3 and HO4 were purified by Talon[®] affinity chromatography.

Figure 4. Spectroscopic characterization of the catalytic activity of the heme-HO complex in the presence of spinach Fd. After addition of an NADPH-regenerating system time dependent absorbance changes were monitored every minute over a period of 30 minutes. HY1 reaction (A) assayed without iron chelator. The ferrous dioxyheme complex was formed [Heme(Fe²⁺)-O₂] (asterisks indicate β -/ α -bands of the complex at 540 nm and 579 nm). A product peak at 670 nm cannot be detected. HO2 (B) is not able to bind heme and after 30 min no spectral changes could be observed. Formation of heme-HO3 complex (C) and heme-HO4 complex (D) was measured in the presence of an iron chelator (desferrioxamine). The directions of spectral changes are indicated by arrows.

Figure 5. Binding of protoporphyrin IX (proto IX) to HO2. Absorption spectra of free (dashed line) and HO2 bound (solid line) proto IX in potassium phosphate buffer pH 7.2 (A). The protein peak at 280 nm and the absorption maximum of bound proto IX at 398 nm were monitored. Gel permeation chromatography was performed with the proto IX-HO2 complex (B). The protein (solid line) and proto IX (dashed line) absorbance were measured. Both HO2 and proto IX eluted at 11.5 ml. The two minor protein peaks at 15 ml and 18 ml were HO2 degradation products without bound proto IX.

Figure 6. HPLC elution profiles of HO metabolites and BV references. HO reaction products were analyzed by reversed-phased HPLC after Sep-Pak preparation. The HY1, HO3, and HO4 reaction products eluted at 20 min. The mixture of BV isomers (α , β , γ , and δ) obtained by chemical oxidative degradation of hemin eluted between 20 and 40 minutes. The commercial (com) BV IX α eluted at 20 min. Absorbance was monitored at 650 nm.

Figure 7. pH and temperature dependence of the HO reactions. The relative activity of HO reactions was calculated by BV formation. The pH optima of HY1, HO3, and HO4 were about pH 7.2 (A). HO3 and HO4 possess an optimal reaction temperature at more than 45°C (B).

Figure 8. Time-dependent spectroscopic monitoring of the HO3-catalyzed conversion of heme to BV. The conversion of heme to BV by HO3 (10 μ M) was followed spectroscopically in the absence (dashed line) and in the presence (solid line) of 5 mM ascorbate. The assay was started by addition of NADPH-regenerating system and monitored for 30 min. Conversion of heme is illustrated by the decrease of the Soret band at 405 nm.

Figure 9. Light dependence of the HO reaction. Light dependence of the HO reaction was observed using isolated thylakoid membranes as an electron donor. The reaction was incubated in the dark (dashed line) or irradiated with light after 100 s (solid line, indicated by arrow) (A). The BV formation was measured at 680 nm. The reaction is shown for HO3. B. The relative HO activity determined as the rate of BV formation at A_{680} was measured for the complete reaction in the light with all assay components (complete), in darkness (dark) and in light in the presence of 50 μ M DCMU or 50 μ M DCMU and reduced 200 μ M DCIP (DCIP) and in the absence of HO (Δ HO) or Fd (Δ Fd). Error bars indicate \pm SE.

Accepted Manuscript

TABLE AND FIGURES

Table 1. Biochemical parameter of HY1, HO3, and HO4.

Parameter	HY1	HO3	HO4
$[mM^{-1} cm^{-1}]$	203	271	175
$K_D [\mu M]$	1,6	2,3	2,8
$K_M [\mu M]$	1,3	2,7	5,7
$E_A [J mol^{-1}]$	36,60	14,78	10,76

FIGURE 1

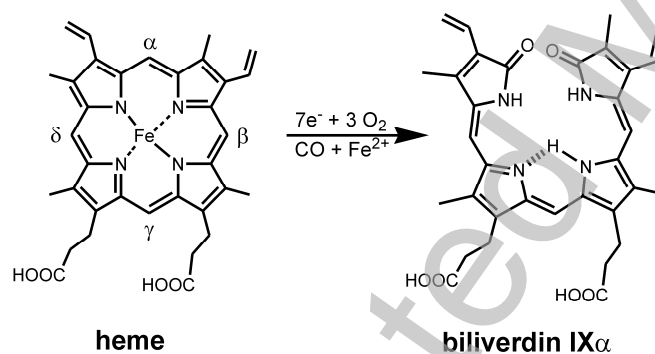
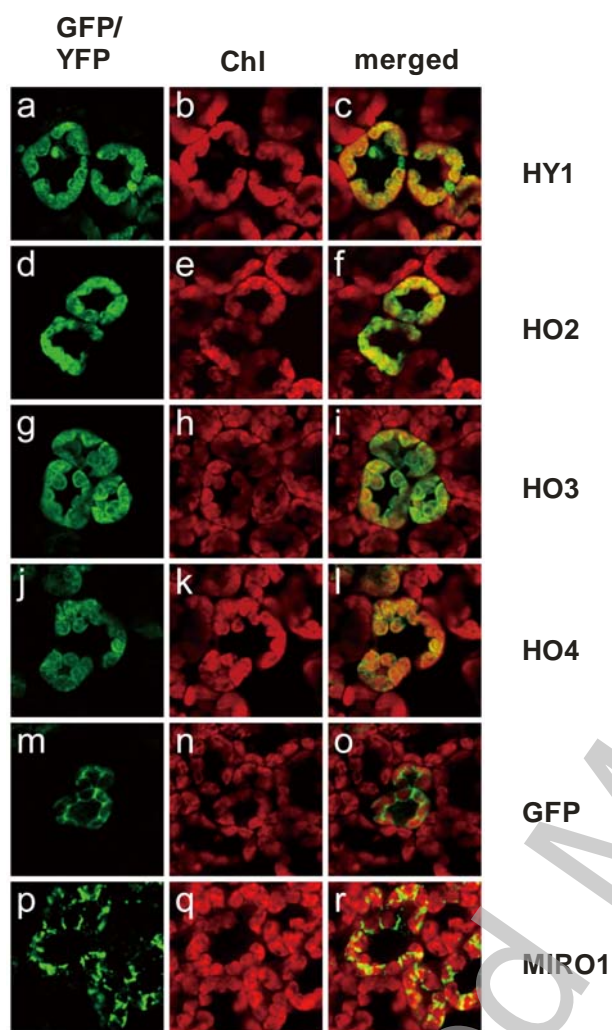


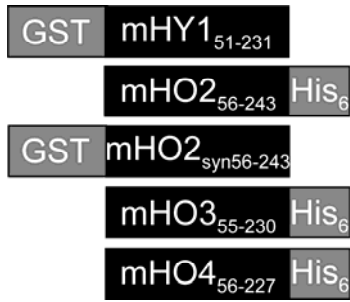
FIGURE 2



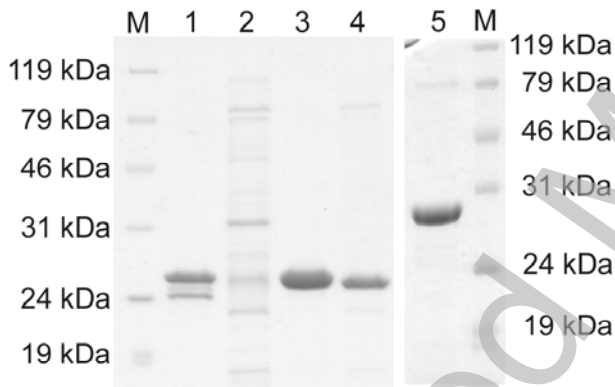
Accepted Manuscript

FIGURE 3

A



B



THIS IS NOT THE VERSION OF RECORD - see doi:10.1042/BJ20090775

Accepted Manuscript

FIGURE 4

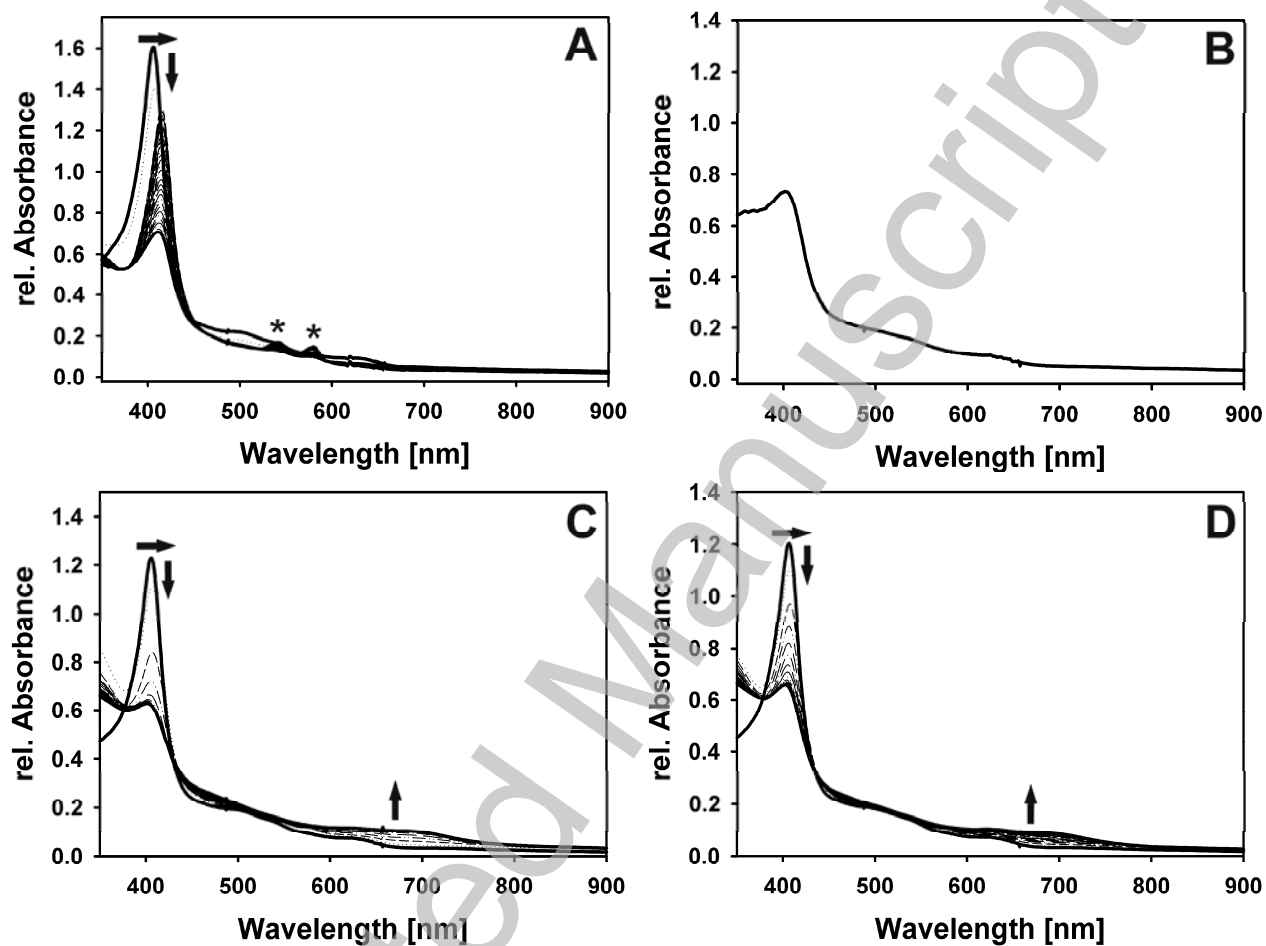
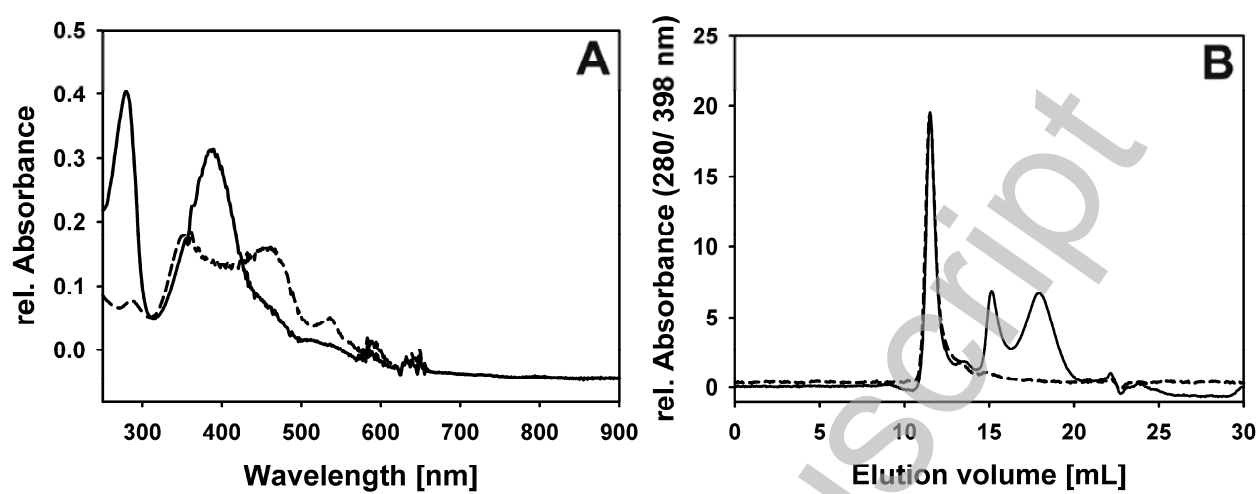


FIGURE 5



THIS IS NOT THE VERSION OF RECORD - see doi:10.1042/BJ20090775

Accepted Manuscript

FIGURE 6

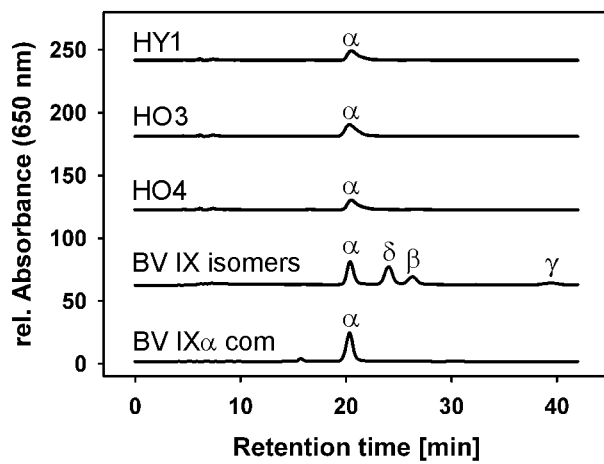
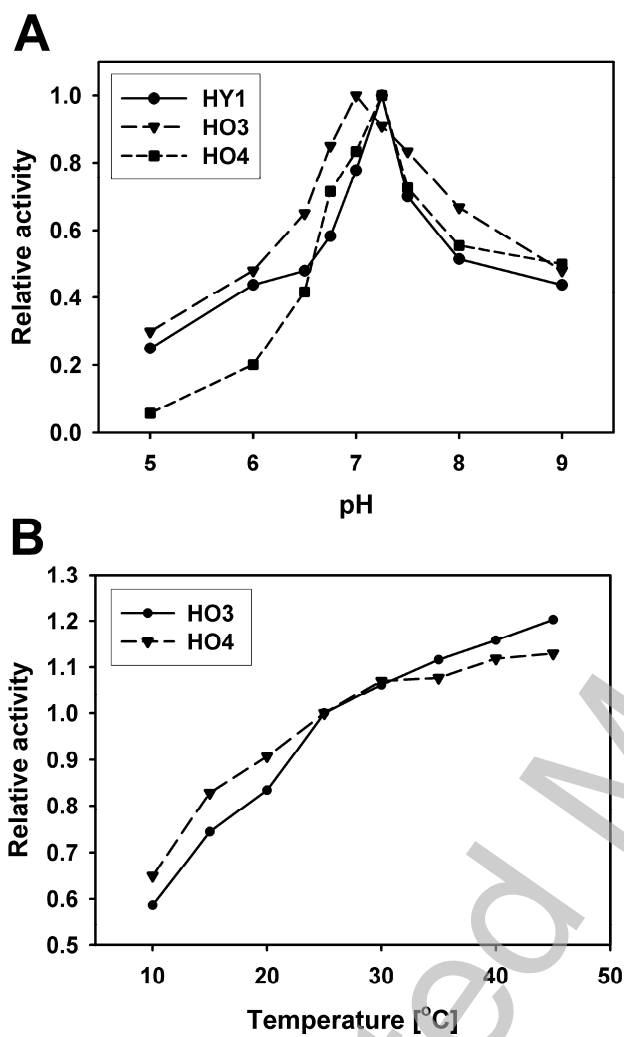


FIGURE 7



THIS IS NOT THE VERSION OF RECORD - see doi:10.1042/BJ20090775

Accepted Manuscript

FIGURE 8

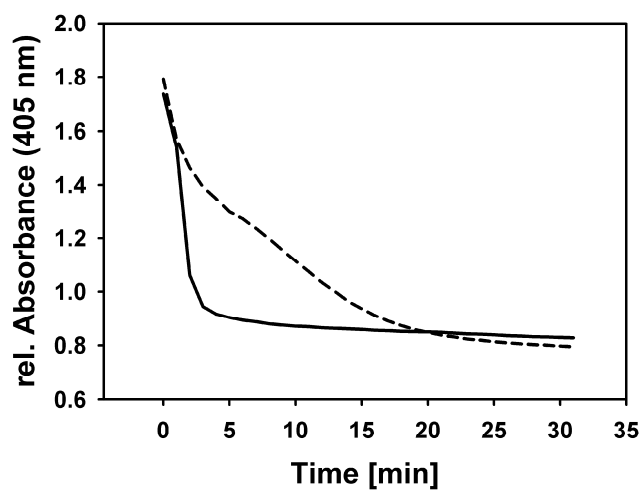
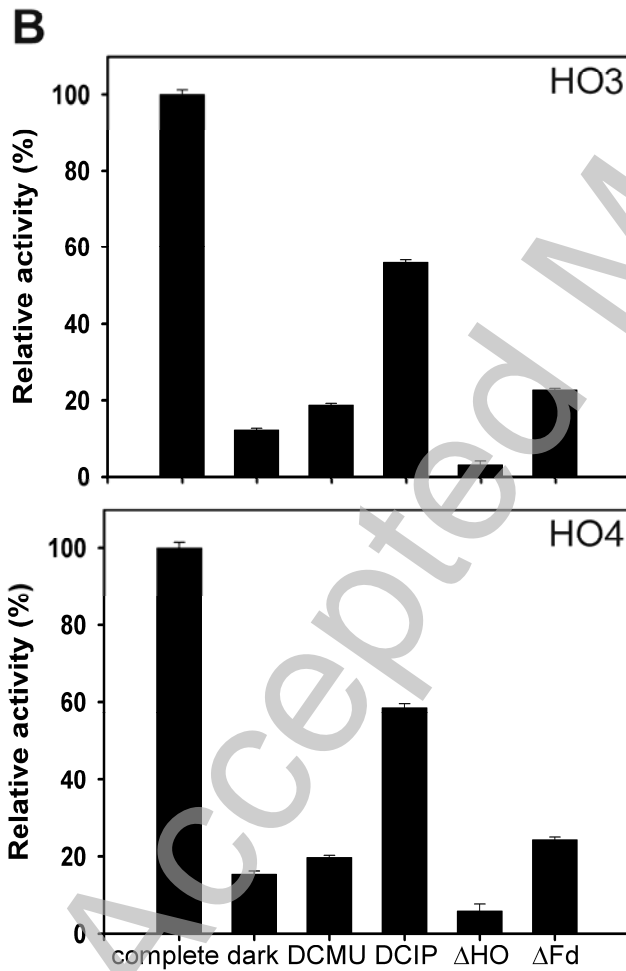
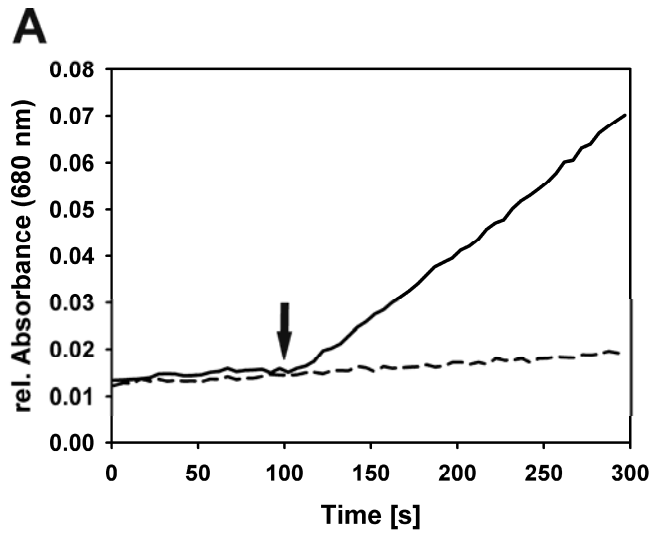


FIGURE 9



THIS IS NOT THE VERSION OF RECORD - see doi:10.1042/BJ20090775